Supporting Information

Brugués et al. 10.1073/pnas.0913669107

SI Text

1 Discussion of the Parameters. In addition to the pipette pressure ΔP, a control parameter in our experiments, the values of the parameters used in the model are listed in Table S1. A range of values for most parameters can be found in the literature and are reported in Table S2. We discuss below how the combinations of parameters relevant to the cell motion can be deduced from our observations (Fig. 5).

1.1 Effective membrane stretching stiffness. Although membrane tension appears to play a marginal role in controlling the cell motion inside the pipette, its influence can be seen in details, such as the saturation of the oscillations (Fig. 5*B*). The effective membrane stiffness to stretching can be estimated by noting that a tongue length of order $L = 30$ μm generates an increase of membrane tension to the point that it might influence cell motion: $\gamma_{\rm mbr} \sim 1$ mN/m, leading to the estimate $k_\gamma \sim 1$ mN/m (the quantitative fit produced $k_\gamma = 0.8$ mN/m). Comparable values were found by analysis of data from refs. 1 and 2. An upper bound for this stiffness is the stretching modulus of the lipid bilayer itself: ≃200 mN/m, Table S2.

1.2 Cortical tension. The Laplace law $\Delta P = 2\gamma(\frac{1}{R_p} - \frac{1}{R})$ can be used to determine the sum of cortical and membrane tensions in micropipette experiments, at static mechanical equilibrium. Although healthy *Entamoeba histolytica* did not display such static equilibrium, one can get an estimate of the cortical tension by noting that our cells managed to retract under pipette suctions larger than $\Delta P = 1$ kPa (Fig. 5). Neglecting the membrane tension and the cell body outside the pipette for this estimate, we find that the cortical tension must be larger than $\Delta P R_p/2 \simeq 2.5$ mN/m. This value is in good agreement with data collected on other amoebae such as *Dictyostelium* (see Table S2). We chose the value $\sigma_{\rm myo} = 5$ kPa, corresponding to a cortical tension $\gamma_{\rm myo} = \sigma_{\rm myo} h = 5$ mN/m for a cortex of thickness $h \simeq 1$ μm (see Sec. 2). This value is slightly larger than the measured cortical tension of *Dictyostelium*, which, unlike *E histolytica*, does not exhibit a strong blebbing activity. The myosin stress can be estimated independently as the product of the stall force of a myosin microfilament $f_{\rm st}$ times the microfilament density in the cortex (of order $1/\xi^2$, given in Table S1). The value $\sigma_{\rm myo} = 5$ kPa corresponds to a myosin microfilament stall force $f_{st} \simeq 12.5$ pN, in good agreement with published data (see Table S2).

1.3 Critical thicknesses. From the observation (Fig. 5) that a cell under a pipette pressure $\Delta P_1 = 1.2$ kPa undergoes cycles of forward and backward motion (oscillatory regime), whereas a cell under pipette pressure $\Delta P_2 = 1.9$ kPa is in the saltatory regime and does never retract, we conclude that the unbinding thickness h_b (independent of pressure) lies in between the (pressure dependent) retraction thicknesses $h_{s,1} = 0.6$ μm and $h_{2,s} = 0.95$ μm, corresponding to ΔP_1 and ΔP_2, respectively (calculated with Eq. **5** of the paper and with $\sigma_{\rm myo} = 5$ kPa). A look to the saltatory regime (Fig. 5) shows that we expect $h_b \lesssim h_{s,2}$. A critical unbinding force $f_b^* = 4.75$ pN, consistent with published data (see Table S2), gives a satisfactory $h_b = 0.95$ μm. In Fig. 3, our interest is to show the effect of the loading rate on membrane detachment, which is best seen for a cortex that does not spontaneously detach under actomyosin contraction ($h_b > h$). To that end, a higher critical unbinding force ($f_b^* = 6$ pN) was chosen for Fig. 3.

The stationary cortex thickness $h = v_p/k_d$ is reached neither in the oscillatory nor in the saltatory regime and thus plays little role in the fitting procedure. The polymerization velocity, however, controls the period of the oscillations τ, which is essentially the time needed to grow a cortex of thickness h_b. We measure $\tau(= h_b/v_p) \simeq 16$ s and deduce a polymerization velocity $v_p \simeq$ 60 nm/s, consistent with the literature (Table S2). Membrane-cortex unbinding is the sign that the stationary cortex thickness is larger than the unbinding thickness, which sets an upper bound on the depolymerization rate: $k_d < v_p/h_b = 1/(15$ s). The value $k_d = 1/(25$ s) was chosen for the fit, giving a stationary thickness $h = 1.5$ μm. Note that the cortex relaxation rate $1/\tau^* = 1/(15$ s) must be larger than the actin depolymerization rate $k_d = 1/$ (25 s), as both actin treadmilling and the kinetics of reorganization of actin cross-linking proteins participate to the cortical stress relaxation.

1.4 Friction parameters. Different types of friction influence the motion of the cell inside the micropipette. Dissipation due to the membrane and cytosolic flows accompanying the cell motion inside the pipette is accounted for in the friction parameter $\eta(L) = \eta_b(1 + L/R_p)$ appearing in Eq. 1, whereas dissipation due to the viscoelastic nature of the cytoskeleton involves the cortex viscosity $E\tau^*$ and the "friction length" L_f (Eq. 2).

The former effect can be quantified from the velocity of the bare membrane tongue inside the pipette upon its detachment from the cortex (of order $\dot{L} = 1.3$ μm/s for a pressure difference $\Delta P = 1.2$ kPa, giving $\eta = \Delta P/\dot{L} \simeq 1$ kPa s/μm). It is thought to mostly originate from the viscous flow of membrane through the dense mesh of cytoskeleton–plasma membrane (CSK-PM) linkers, for which one expects $\eta_b \sim \mu_b/\xi^2$ (3). The effective membrane viscosity μ_b includes membrane friction with the pipette walls, and ξ is the average distance between CSK-PM linkers. The value $\eta_b = 130$ Pa s/μm deduced from our experiment predicts an effective viscosity ($\mu_b = 6.25\ 10^{-7}$ Pa m s) in agreement with published data (see Table S2).

The friction related to cortical flow can be estimated from the retraction velocity of the membrane tongue. For the fit of Fig. 5, we have made the simplifying assumptions that the cortex is in the viscous regime during retraction, in which case the cortex viscoelasticity (given in Eq. 2) amounts to an additional friction term of order $(2Eh\tau^*)/(RpLf)\dot{L}$. The measured retraction velocity ~0.5 μm/s predicts that the cortical friction should be of the same order of magnitude as the friction from membrane flow, consistent with a friction length $L_f \simeq 10$ μm.

2 Determination of the Cortex Thickness. The filamentous actin (F-actin) cytoskeleton of *E. histolytica* seen by fluorescence microscopy (Fig. S1) shows evidence of an F-actin enriched zone of thickness of order 1 μm underneath the plasma membrane. The image was obtained using F-actin staining Lifeact peptide (MGVADLIKKFESISKEE) (4), fused to GFP through a heptapeptide (GDPPVAT). This was achieved by PCR amplification using two oligonucleotides based on *E. histolytica* codon usage:

AT**GGTACC**ATGGGAGTTGCTGATCTTATTAAAAAATT CGAATCAATTTCAAAAGAAGAAG and AT**GGTACC**AGT AGCAACTGGTGGATCTC CTTCTTCTTTTGAAATTGATT CG The PCR fragment cleaved with *Kpn*I-*Bam*HI was cloned into vector pNeo-GFP and transfected into cells. Observation was made with a 60× Olympus objectif (NA = 1.25) on an inverted IX-70 Olympus microscope. Fluorescence imaging was performed with a CoolSNAP HQ2 (Roper Scientific) CCD camera with the Micro-Manager software.

1. Merkel R, et al. (2000) A micromechanic study of cell polarity and plasma membrane cell body coupling in dictyostelium. *Biophys J* 79:707–719.
2. Rentsch P, Keller H (2000) Suction pressure can induce uncoupling of the plasma membrane from cortical actin. *Eur J Cell Biol* 79:975–981.
3. Brochard-Wyart F, Borghi N, Cuvelier D, Nassoy P (2006) Hydrodynamic narrowing of tubes extruded from cells. *Proc Natl Acad Sci USA*103:7660–7663.
4. Riedl J, et al. (2008) Lifeact: A versatile marker to visualize f-actin. *Nat Methods* 5:605–607.

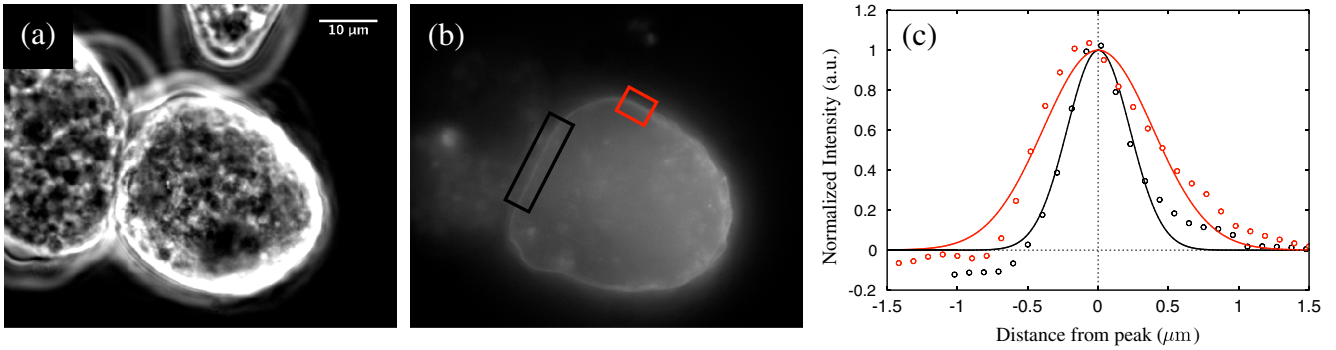

Fig. S1. (*a*) Phase contrast image and (*b*) fluorescent image of *E. histolytica* transfected for expressing the F-actin binding peptide LifeAct coupled to GFP (see text). (*c*) Fluorescence intensity plot (after subtraction of the background fluorescence intensity, and along with Gaussian fits) showing an F-actin-cortical region of thickness of order 1 μm beneath the plasma membrane. The data points are taken from the region inside the colored boxes in *b*, and the Gaussian fits produce a width at half maximum $h = 0.5$ μm (black) and $h = 1$ μm (red).

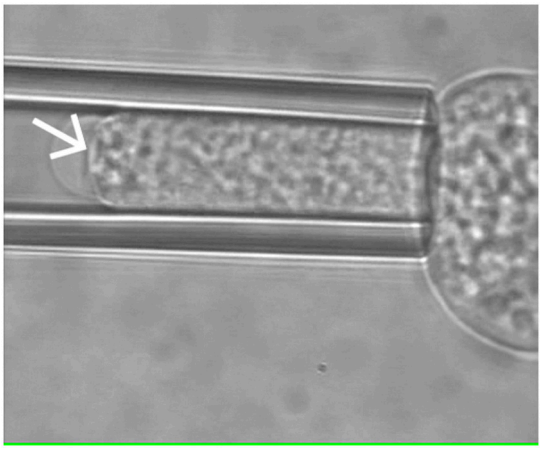

Movie S1. Saltatory regime (accelerated 5 times). Movie of the motion of an *E. histolytica* cell subjected to micropipette suction (pipette radius 5 μm, pipette pressure $\Delta P = 1.9$ kPa). This cell is initially in the saltatory regime. Two rupture events can be seen (white arrows), where the membrane detaches from the cytoskeleton cortex and jumps forward. After the first rupture, the membrane tongue is seen to slow down and almost stall due to cortex repolymerization. After the second rupture, a transition to a steady flow regime is then observed (possibly due to the increasing pipette radius), where aborted attempts of cortex repolymerization only manage to transiently slow down part of the membrane tongue (yellow arrows).
Movie S1 (MOV)

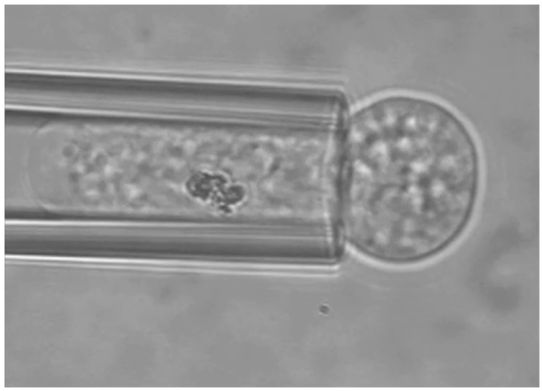

Movie S2. Oscillatory regime (accelerated 20 times). Movie of the motion of an *E. histolytica* cell subjected to micropipette suction (pipette radius 5 μm, pipette pressure $\Delta P = 1.2$ kPa). After a transient regime, this cell settles in the oscillatory regime, where events of membrane detachment and fast-forward motion alternate with membrane retraction caused by cortex repolymerization and contraction. After 15 periodic oscillations, the cell also ends up being swallowed by the pipette.
Movie S2 (MOV)

Table S1. Values of the parameters used to calculate the cell motion in Fig. 5

Membrane parameters	
Membrane tension at rest	$\gamma_0 \simeq 0$ (irrelevant)
Membrane stretching modulus	$k_\gamma = 0.8$ mN/m
Effective membrane friction	$\eta_b = 130$ Pa.s/μm
Critical unbinding force	$f_b^* = 4.75$ pN
Geometric parameters	
Pipette radius	$R_p = 5$ μm
Cell unperturbed radius	$R_0 = 15$ μm
Cortex parameters	
Cortex mesh size	$\xi = 50$ nm
Actin polymerization velocity	$v_p = 60$ nm/s
Actin depolymerization rate	$k_d = 1/(25\ \mathrm{s})$
Cortex Young's modulus	$E = 1$ kPa
Cortex relaxation time	$\tau^* = 15$ sec
Myosin stress	$\sigma_{\mathrm{myo}} = 5$ kPa
Friction length	$L_f = 10$ μm

Table S2. Expected value of the parameters from the literature

Cortical tension	$\gamma_{myo} = \sigma_{myo} h = 10^{-5} - 4.10^{-3}$ J/m^2	(In *Dictyostelium*) (1–3)
Cortex thickness	$h \simeq 1$ μm	Sec. 2
Membrane stretching modulus	$k_\gamma = 0.1$–200 mN/m	Calculated from refs. 4–6
Membrane viscosity	$\mu_b (= \eta_b \xi^2) = 10^{-8} - 10^{-4}$ Pa.m.s	(7)
Cortex Young's modulus	$E = 10^2$–10^3 Pa	(8)
Cortex relaxation time	$\tau^* = 0.01$–100 s	(9)
Polymerization velocity	v_p: up to 10 μm/ min	(10)
Cortex mesh size	$\xi = 20$–200 nm	(11)
Myosin Microfilament stall force	$f_{st} = 5$–20 pN	(12)
Critical unbinding force	$f_b^* = 1$–10 pN	(13)

1. Pasternak C, Spudich JA, Elson, EL (1989) Capping of surface receptors and concomitant cortical tension are generated by conventional myosin. *Nature* 341:549–551.
2. Egelhoff TT, Naismith TV, Brozovich FV (1996) Myosin-based cortical tension in dictyostelium resolved into heavy and light chain-regulated components. *J Muscle Res Cell Mot* 17:269–274.
3. Dai J, Ping Ting-Beall H, Hochmuth RM, Sheetz MP, Titus MA (1999) Myosin 1 contributes to the generation of resting cortical tension. *Biophys J* 77:1168–1176.
4. Merkel R, et al. (2000) A micromechanic study of cell polarity and plasma membrane cell body coupling in dictyostelium. *Biophys J* 79:707–719.
5. Rentsch P, Keller H (2000) Suction pressure can induce uncoupling of the plasma membrane from cortical actin. *Eur J Cell Biol* 79:975–981.
6. Evans E, Rawicz W (1990) Entropy-driven tension and bending elasticity in condensed-fluid membranes. *Phys Rev Lett* 64:2094–2097.
7. Brochard-Wyart F, Borghi N, Cuvelier D, Nassoy P (2006) Hydrodynamic narrowing of tubes extruded from cells. *Proc Natl Acad Sci USA* 103:7660–7663.
8. Stricker J, Falzone T, Gardel ML (2010) Mechanics of the f-actin cytoskeleton. *J Biomech* 43:9–14.
9. Balland M, et al. (2006) Power laws in microrheology experiments on living cells: Comparative analysis and modeling. *Phys Rev E* 74:021911.
10. Pollard TD, Borisy GG (2003) Review cellular motility driven by assembly and disassembly of actin filaments. *Cell* 112:453–465.
11. Morone N, et al. (2006) Three-dimensional reconstruction of the membrane skeleton at the plasma membrane interface by electron tomography. *J Cell Biol* 174:851–862.
12. Oiwa K, Chaen S, Kamitsubo E, Shimmen T, and Sugi H (1990) Steady-state force-velocity relation in the ATP-dependent sliding movement of myosin-coated beads on actin cables in vitro studied with a centrifuge microscope. *Proc Natl Acad Sci USA* 87:7893–7897.
13. Evans E (2001) Probing the relation between force—lifetime—and chemistry in single molecular bonds. *Annu Rev Bioph Biom* 30:105–128.